Chemical Engineering & Processing: Process Intensification 165 (2021) 108450

Contents lists available at ScienceDirect

Chemical Engineering and Processing - Process Intensification

journal homepage: www.elsevier.com/locate/cep

# Experimental study of $CO_2$ absorption with MEA solution in a novel Arc-RPB

Vahid Mohammadi Nouroddinvand, Amir Heidari *

*Process Simulation and Modeling Laboratory (PSMlab), Faculty of Chemical, Petroleum and Gas Engineering, Semnan University, Semnan, 3513119111, Iran*

ARTICLE INFO

*Keywords:*
Arc-blade rotating packed bed (Arc-RPB)
Process intensification (PI)
$CO_2$ absorption
Mono-ethanol-amine (MEA)

ABSTRACT

In this research, a new design of high-gravity (HiGee) Arc-blade Rotating Packed Bed (Arc-RPB) was introduced to study the Arc-RPB effect on carbon dioxide ($CO_2$) absorption efficiency with Mono-Ethanol-Amine (MEA) aqueous solution. The effect of packing rotational speed, gas to liquid inlet flow ratios, MEA and $CO_2$ concentrations were studied on absorption efficiency of the Arc-RPB. Experimental results showed that an increase in the rotational speed of Arc-RPB from 300 rpm to 900 rpm enhances $CO_2$ absorption efficiency about 9% and 3% for 1 M and 2 M MEA solution, respectively. Also, experiments indicated that an increase in the gas to liquid flow ratio decreases $CO_2$ absorption efficiency about 5% at different MEA solution concentrations. With the study of $CO_2$ inlet concentration from 5000 ppm to 20,000 ppm, it was found that absorption efficiency enhances about 10% in the Arc-RPB. Experimental work showed that by enhancing MEA solution concentration from 0.5 M to 1 M, absorption efficiency increases about 23%, but an increase in MEA solution concentration from 1 M to 2 M enhances efficiency less than 3%. Also, based on experimental data and genetic algorithm (GA) optimization method, a correlation was proposed to predict gas-phase volumetric mass transfer coefficient ($k_G a$) in the Arc-RPB.

## 1. Introduction

Concerns about increase $CO_2$ concentration in the atmosphere as the most important greenhouse gas have paved the way for the development of $CO_2$ capturing and storage technologies. Unfortunately, anthropogenic sources of $CO_2$ emissions are very different, but the power generation sector has the main contribution, about 41% [1] in $CO_2$ emission between all sources. This large amount of $CO_2$ generation is due to fossil fuel combustion (e.g. coal, oil, and natural gas) in the power plants and electricity generation process. In addition, the portion of industries and transportation activities in $CO_2$ emission are equal and about 24% for each one. While the building sector role in $CO_2$ emission is around 8% [1]. It is worth mentioning that a 500 MW power plant with coal fuel produces about 8000–10,000 tons of $CO_2$ per day and a similar capacity combined cycle power plant (gas fuel) produces about 4000 tons of $CO_2$ per day [2].

Today, development and modification in absorption processes can be a practical method to reduce $CO_2$ emission in the world. The developed technologies to capture $CO_2$ can be classified into three approaches as 1) Pre-Combustion, 2) Oxy-Combustion, and 3) Post-combustion [3,4]. In pre-combustion $CO_2$ capture, there is a reaction between a fuel and oxygen/air to give mainly a fuel gas, generally $CO$ and $H_2$. Carbon monoxide ($CO$) is reacted with steam in a catalytic reactor, to give $CO_2$ and more $H_2$. Then, the $CO_2$ is removed by one of the absorption/adsorption or membranes process that results high $H_2$ concentration stream [5,6]. In Oxy-combustion, fuel is combusted with the oxygen that is diluted with recycled flue gas rather than air. This oxygen-rich atmosphere results in final flue gases consisting mainly of $CO_2$ and $H_2O$, producing a more concentrated $CO_2$ flow for easier purification [7]. The post-combustion process is the capture of $CO_2$ from the combustion of fossil fuels or other carbonaceous groups [8,9]. In this process, the thermodynamic driving force from gas streams is low because the concentration of $CO_2$ is less than 15% [3]. The post-combustion capture process is the most method to capture and storage of $CO_2$ [3,10].

For reduction of $CO_2$ concentration from the gas phase, conventional absorption columns such as packed beds have been used in chemical industries. The main problem of packed beds is the large size of the bed column that significantly increases the capital and operating costs [11–13]. In contrast, the use of Rotating Packed Beds (RPBs) can be effective in reducing the size of the equipment and decrease of operating costs [11–13]. Hopes to reduce $CO_2$ concentration increased with

* Corresponding author.
*E-mail address:* amirheidari@semnan.ac.ir (A. Heidari).

https://doi.org/10.1016/j.cep.2021.108450
Received 20 October 2020; Received in revised form 10 April 2021; Accepted 28 April 2021
Available online 7 May 2021

**Nomenclatures**

| | |
|---|---|
| $a$ | Gas-liquid interfacial area ($m^2/m^3$) |
| $a_c$ | Centrifugal acceleration ($m/s^2$), $a_c = \omega^2 r$ |
| $a_t$ | Effective surface area of the bed ($m^2/m^3$), $a_t = A_{mesh} / V_{reactor}$ |
| $C_1$ | $CO_2$ concentration at the gas outlet ($mol/m^3$) |
| $C_2$ | $CO_2$ concentration at the gas inlet ($mol/m^3$) |
| $D_{CO_2-solution}$ | $CO_2$ diffusion coefficient into solution ($m^2/s$) |
| $d_p$ | Effective diameter of the packing (m), $d_p = 6(1-\varepsilon)/a_t$ |
| $E$ | Efficiency (%) |
| $Gr_G$ | Gas phase Grashof number, $Gr_G = \rho_G^2 a_c d_p^3/\mu_G^2$ |
| $h$ | Axial height of the packing (m) |
| $k_G a$ | Gas side volumetric mass transfer coefficient ($1/s$) |
| $Q_G$ | Gas flow rate ($m^3/s$) |
| $Q_L$ | Liquid flow rate ($m^3/s$) |
| $r_{mean}$ | Average radius of packing ($m$), $r_{mean} = \sqrt{(R_1^2+R_2^2)/2}$ |
| $R$ | RPB bed radius ($m$) |
| $Re_G$ | Gas phase Reynolds number, $Re_G = \rho_G Q_G d_p/(2\pi r_{mean} h)\mu_G$ |
| $Re_L$ | Liquid phase Reynolds number, $Re_L = \rho_L Q_L d_p/(2\pi r_{mean} h)\mu_L$ |
| $R_1$ | Inner radius of the packing ($m$) |
| $R_2$ | Outer radius of the packing ($m$) |
| $V_{mesh}$ | Volume of the packing mesh ($m^3$) |
| $V_{reactor}$ | Volume of the reactor ($m^3$) |
| $We_L$ | Liquid phase Weber number, $We_L = \rho_L Q_L^2 d_p/(2\pi r_{mean} h)^2 \sigma$ |
| $x_{in,MEA}$ | MEA mole fraction in the liquid inlet |
| $y_{in,CO_2}$ | $CO_2$ mole fraction in the gas inlet |

*Greek symbols*

| | |
|---|---|
| $\varepsilon$ | Voidage (Dimensionless) |
| $\mu_G$ | Gas viscosity ($Pa.s$) |
| $\mu_l$ | Liquid viscosity ($Pa.s$) |
| $\rho_G$ | Gas density ($kg/m^3$) |
| $\rho_L$ | Liquid density ($kg/m^3$) |
| $\sigma$ | Surface tension ($N/m$) |
| $\omega$ | Angular velocity ($rad/s$) |

presentation of RPB reactors as a process intensification by Ramshaw and Mallinson [14]. After the presenting of the first RPB prototype by Ramshaw and Mallinson [14], more advanced prototypes of RPBs were quickly developed for various applications by researchers. Use of the RPBs in $CO_2$ capturing [2,15–17], $H_2S$ and $SO_2$ absorption from flue gas [18–21] and other applications such as micro-mixing [22,23], Distillation [24], Extraction [25], synthesis of Nano-particle [26–29] showed the very good potential of RPBs to increase chemical process efficiency.

In recent years, numerous investigations have been carried out in laboratory scale RPBs to determine the effect of design and operating parameters on absorption performance of $CO_2$ by RPBs. Wang and Chen [17] studied the effects of different alkanolamine solutions on the $CO_2$ removal efficiency at various lean and high $CO_2$ loadings in a RPB. Their experimental results showed that increasing the alkanolamine concentration enhances the $CO_2$ absorption efficiency. Chen et al. [30] provided an integrated approach for air pollution reduction (e.g. $CO_2$, $SO_2$, $NO_x$, and total suspended particulates (TSP)) with coal fly ash (CFA) in a RPB. Their results indicated that the maximum removal efficiencies for $CO_2$, $SO_2$, $NO_x$, and TSP were 96.3 ± 2.1%, 99.4 ± 0.3%, 95.9 ± 2.1%, and 83.4 ± 2.6%, respectively. Also, energy consumption for absorption capacity of 510 kg $CO_2$/day was evaluated about 112 kWh/$t$-$CO_2$. Lu et al. [31] studied the single-layer hydrophobic surface-modified stainless steel wire mesh (SSM) and nonsurface-modified stainless steel wire mesh (NSM) on the gas-liquid interfacial area in the RPB. Comparison of liquid dispersion cone angle between rotating single-layer SSM and NSM shows that SSM is suitable for the initial liquid dispersion in RPB. The experimental results showed that the interfacial area in the RPB with SSM packing was higher than NSM packing, demonstrating the influence of initial liquid dispersion on the mass transfer performance. Zhang et al. [32] investigated the physical $CO_2$ absorption with an ionic liquid (IL) in a RPB. They found that only a contact cycle in the RPB can make the saturation ratio of $CO_2$ until 60%. Furthermore, they studied the effects of various operation conditions on the liquid side volumetric mass transfer coefficient ($k_L a$). Their results showed that $k_L a$ value in the RPB is at least one order of magnitude higher conventional packed bed towers. Also, they proposed a model with a deviation of less than 15% to describe the $k_L a$. Borhani and Wang [2] studied the effect of solvents selection on the $CO_2$ absorption process in the RPB. They classified $CO_2$

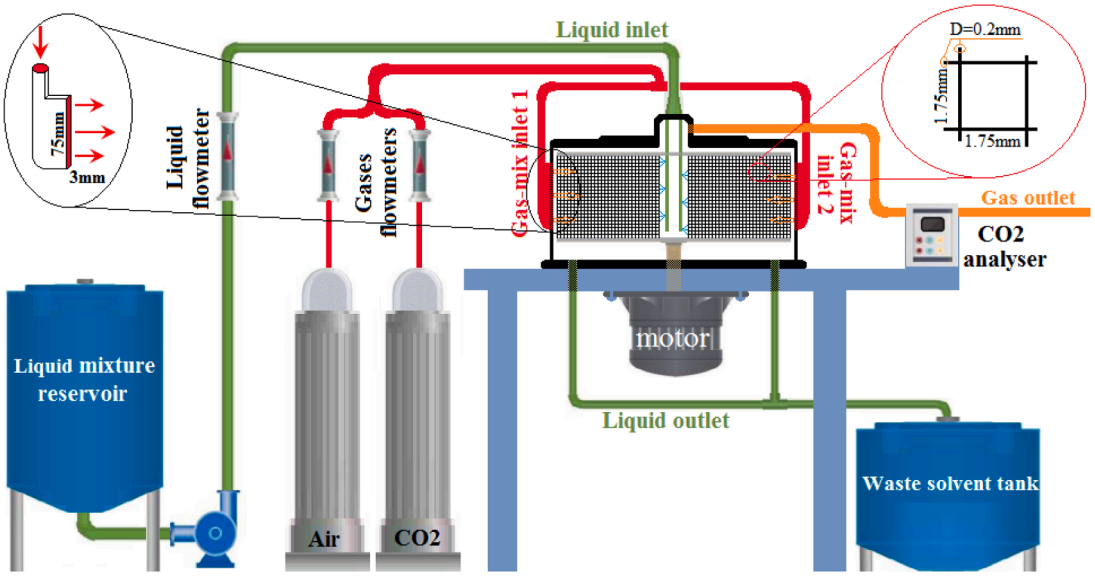


**Fig. 1..** Schematic of Arc-RPB setup.

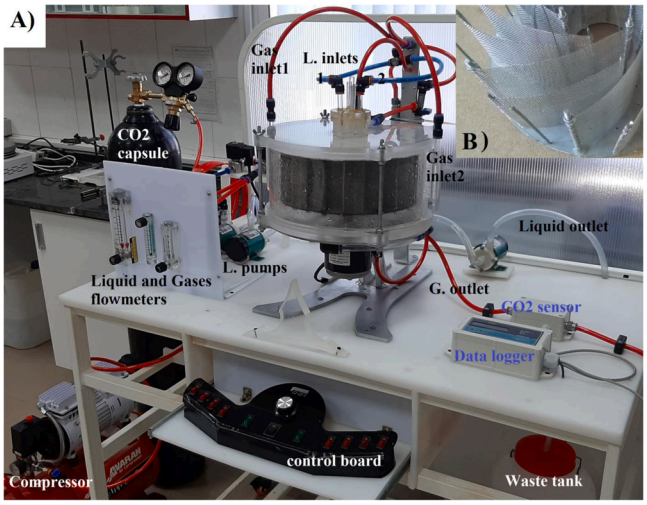


**Fig. 2..** A) Experimental setup of Arc-RPB and B) Packing of Arc-RPB.

**Table 1**
Structural dimensions of the Arc-RPB.

| | |
|---|---|
| Radius of Arc-RPB ($R$) | 0.155 m |
| Inner radius of the packing ($R_1$) | 0.04 m |
| Outer radius of the packing ($R_2$) | 0.14 m |
| Axial height of the packing ($h$) | 0.098 m |
| Volume of the packing | 5542 $cm^3$ |
| Liquid distributor | 6 Pcs, $D = 1$ mm |
| Porosity ($\varepsilon$) | 0.9882 |
| Effective surface area ($a_t$) | 53.5 $m^2/m^3$ |

capture process as chemical, physical, and chemical-physical absorption. They reported that the efficiency and the process costs directly affected by the solvent, due to solvent effect on $CO_2$ absorption capacity, size of equipment, and solvent regeneration energy.

Against this backdrop, the present study is focused on developing a new RPB design as the Arc-RPB to increase absorption efficiency of $CO_2$ by MEA in RPBs. To the best of our knowledge, no study has been reported regarding the effect of Arc-blade meshes for RPBs. In order to show the performance of the Arc-RPB, an experimental setup has been developed. The Arc-RPB performance is evaluated at different experimental conditions, including gas and liquid flow rates, MEA solution and $CO_2$ concentrations and rotation speed of RPB. Also, the Genetic Algorithm (GA) method has been used to develop an empirical correlation to account for gas side volumetric mass transfer coefficient ($k_G a$) as a function of dimensionless numbers.

## 2. Experimental work

### 2.1. Arc-RPB geometrical details

In this research, a novel rotating packed bed reactor (RPB) with Arc-blades was introduced as Arc-RPB for $CO_2$ absorption by MEA. Fig. 1 shows the schematic of the Arc-RPB, and Fig. 2 depicts the experimental setup in the current study. In the Arc-RPB, the packed bed was made with stainless steel arch meshes with the same radius (135 mm) in two layouts. The meshes have a square style with a 1.75 mm length and width. The first layout begins from the inner radius of Arc-RPB to the outer radius, and the second layout starts from a radius of 75 mm to the outer edge of the bed (Fig. 2B). In addition, instead of the usual circular designs of gas inlet, a new design was proposed to direct the gas stream uniformly to the RPB. The two gas inlets were in rectangle shape with dimensions of 3 mm in width and 75 mm length in the axial direction and they were located opposite each other in the reactor body (Fig. 1). The two liquid distributors were placed in the center of the reactor with the angle of 45° with respect to the gas inlets. In the current Arc-RPB, fluids were in counter-current contact with each other. Liquid and gas flow rates were adjusted by flowmeters and rotameters. Also, $CO_2$ meter with accuracy of 10 ppm was used to measure $CO_2$ at inlet and outlet streams. Table 1 shows structural specifications of the Arc-RPB in this work.

### 2.2. Materials

The materials of experimental work included MEA solution and $CO_2$ mixture. The MEA solutions were prepared at 0.5-2 Molar with distilled water and $CO_2$ gas mixtures were prepared at 5000-20,000 ppm to do experimental studies. The MEA was supplied from Shazand Petrochemical industries with 99% purity and a high-pressure capsule of $CO_2$ with 99.99% purity was used during the experiments.

## 3. Results and discussion

### 3.1. Mechanism of $CO_2$ absorption with MEA

The reactions between $CO_2$ and MEA solution has been described by two mechanisms; the zwitterion mechanism [33] and the termolecular mechanism [34]. According to Aboudheir et al. [35] $CO_2$ reaction with MEA in the aqueous solution can be described by the following reactions:

Ionization of water:

$$2H_2O \leftrightarrow OH^- + H_3O^+ \quad (1)$$

Dissociation of dissolved $CO_2$ to carbonic acid:

$$CO_2 + 2H_2O \leftrightarrow HCO_3^- + H_3O^+ \quad (2)$$

Bicarbonate dissociation as:

$$HCO_3^- + H_2O \leftrightarrow CO_3^{2-} + H_3O^+ \quad (3)$$

Zwitterion formation from reaction of MEA with $CO_2$:

$$CO_2 + RNH_2 \leftrightarrow RNH_2^+ COO^- \quad (4)$$

Deprotonation of the zwitterion and carbamate formation:

$$RNH_2^+ COO^- + RNH_2 \leftrightarrow RNH_3^+ + RNHCOO^- \quad (5)$$

$$RNH_2^+ COO^- + H_2O \leftrightarrow H_3O^+ + RNHCOO^- \quad (6)$$

$$RNH_2^+ COO^- + OH^- \leftrightarrow H_2O + RNHCOO^- \quad (7)$$

Carbamate reversion to bicarbonate (hydrolysis reaction):

$$RNHCOO^- + H_2O \leftrightarrow RNH_2 + HCO_3^- \quad (8)$$

Dissociation of protonated MEA:

$$RNH_3^+ + H_2O \leftrightarrow RNH_2 + H_3O^+ \quad (9)$$

Bicarbonate formation:

$$CO_2 + OH^- \leftrightarrow HCO_3^- \quad (10)$$

The absorption of $CO_2$ using MEA is a pseudo-first-order reaction dominated by molecular diffusion, physical dissolution and chemical reaction [36]. According to Aroonwilas et al. [37], the chemical reaction of $CO_2$ with MEA is very fast and $CO_2$ converts to other components as soon as it is physically absorbed in the liquid phase. Therefore, it can be concluded that the main resistance in the mass transfer mechanism is penetration of $CO_2$ from the gas phase to the gas-liquid.

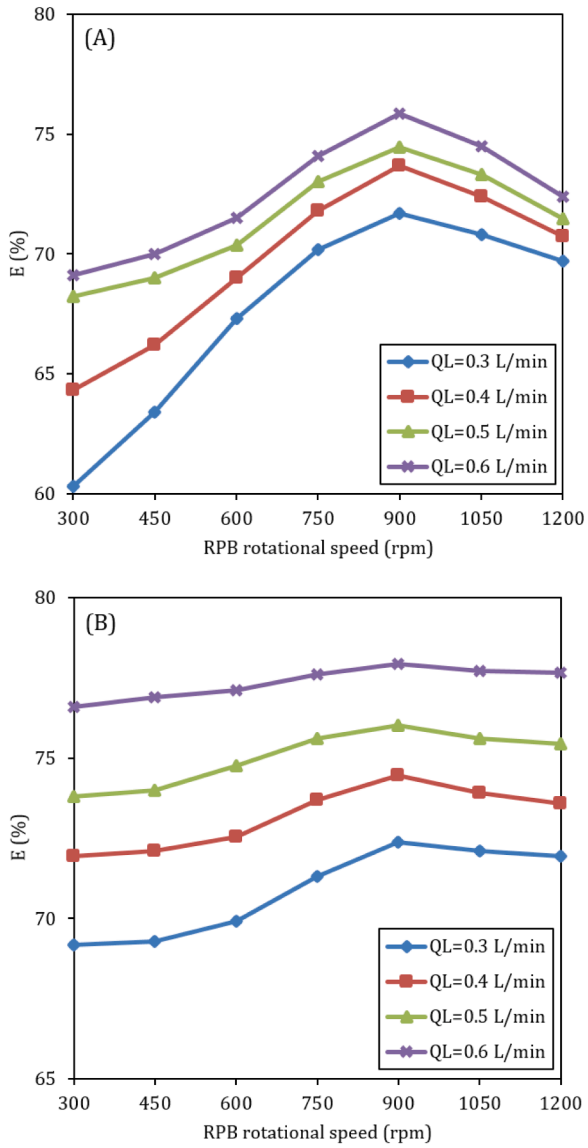


**Fig. 3..** Effect of rotational speed and liquid phase flow rate on $CO_2$ absorption efficiency **A)** MEA solution concentration = 1 M ($Q_G$ = 56 L/min and $CO_2$ inlet concentration = 20,000 ppm) **B)** MEA solution concentration = 2 M ($Q_G$ = 56 L/min and $CO_2$ inlet concentration = 20,000 ppm).

### 3.2. Effect of rotational speed on $CO_2$ absorption

Fig. 3A and B show the effect of Arc-RPB rotational speed (300–1200 rpm) on $CO_2$ absorption efficiency at different flow rates and concentrations of MEA solution. The $CO_2$ absorption efficiency $E$ is calculated by the following equation:

$$E = \frac{C_2 - C_1}{C_2} \times 100 \quad (11)$$

where $C_2$ and $C_1$ are $CO_2$ concentrations at gas inlet and outlet, respectively.

Fig. 3A and B depict at the constant liquid flow rate, increase in rotational speed of Arc-RPB from 300 to 900 rpm enhances $CO_2$ absorption efficiency. The absorption efficiency increase was about 9% for 1 M solution and about 3% for 2 M solution. Enhancement in rotational speed generates smaller droplet sizes due to stronger centrifugal force, leading to a more contact surface area between gas and liquid phases and enhances absorption efficiency. Also, Fig. 3A and B depict the 2 M MEA solution absorption efficiency compared to the 1 M solution. With

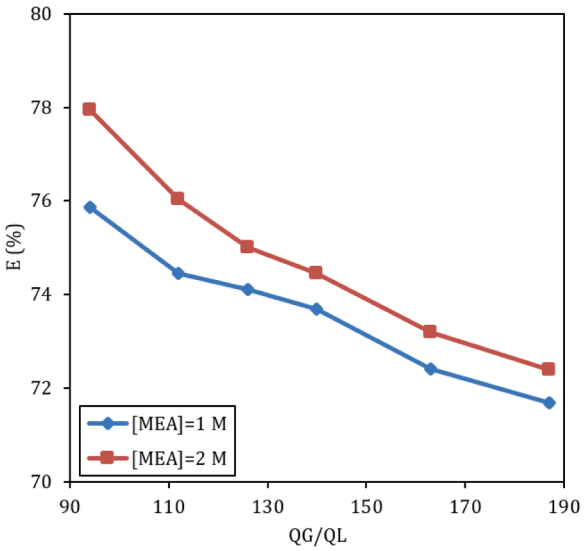


**Fig. 4..** Effect of gas-liquid flow ratio ($Q_G/Q_L$) at different MEA solution concentration on $CO_2$ absorption efficiency (RPB rotational speed = 900 rpm and $CO_2$ concentration = 20,000 ppm).

the rise in MEA solution concentration, solution viscosity enhances which causes higher residence time of liquid phase in the Arc-RPB compared to the 1 M solution (positive effect in $CO_2$ absorption efficiency). At the same time, the higher viscosity of the 2 M solution with respect to the 1 M solution decreases the surface tension of the liquid phase that it leads to larger droplets size of the 2 M solution compared with 1 M solution in the same rotational speeds (negative effect in $CO_2$ absorption efficiency). Based on the laboratory data results, it was concluded that the positive effect (increase in residence time) prevails over the adverse impact (decrease in the gas-liquid interfacial area); as a result, enhancement in MEA solution concentration increases absorption efficiency.

Fig. 3 shows an increase in rotational speed from 900 rpm to 1200 rpm at the 1 M and 2 M solutions of MEA decreases $CO_2$ absorption efficiency. It seems that for rotational speeds higher than 900 rpm, the negative effect of reduction in liquid residence time overcomes the positive impact of the increase in the gas-liquid interfacial area for the mass transfer mechanism. Consequently, absorption efficiency decreases at high rotational speeds. Furthermore, results show in the 2 M MEA solution, due to the higher viscosity with respect to the 1 M solution, the absorption efficiency depicts less sensitivity to the rotational speed (less than 1%), while for the 1 M MEA solution, it is about 3%.

### 3.3. Effect of gas to liquid volumetric flow rate ratio on $CO_2$ absorption

Fig. 4 shows the effect of gas to liquid volumetric flow rate ratio ($Q_g/Q_l$) on the $CO_2$ absorption efficiency. The MEA solution was prepared at the 1 M and 2 M concentration, and rotational speed was adjusted at 900 rpm. Experimental results showed that changing the gas to liquid flow rate ratio plays a vital role in $CO_2$ absorption from the gas phase. Increase in liquid flow rate, which is equal to a decrease in the $Q_g/Q_l$ ratio increases the liquid phase holdup and the gas-liquid interfacial area of MEA solution at the packing surface that provides more absorption efficiency of $CO_2$ at the RPB. Conversely, an increase in the $Q_g/Q_l$ ratio reduces residence time of the gas phase and wetting efficiency in the bed, which causes a reduction in the RPB efficiency. As Fig. 4 depicts an increase in the $Q_g/Q_l$ ratio from 94 to 187 decreases $CO_2$ absorption efficiency about 4% and 6% for 1 M and 2 M MEA solution, respectively.

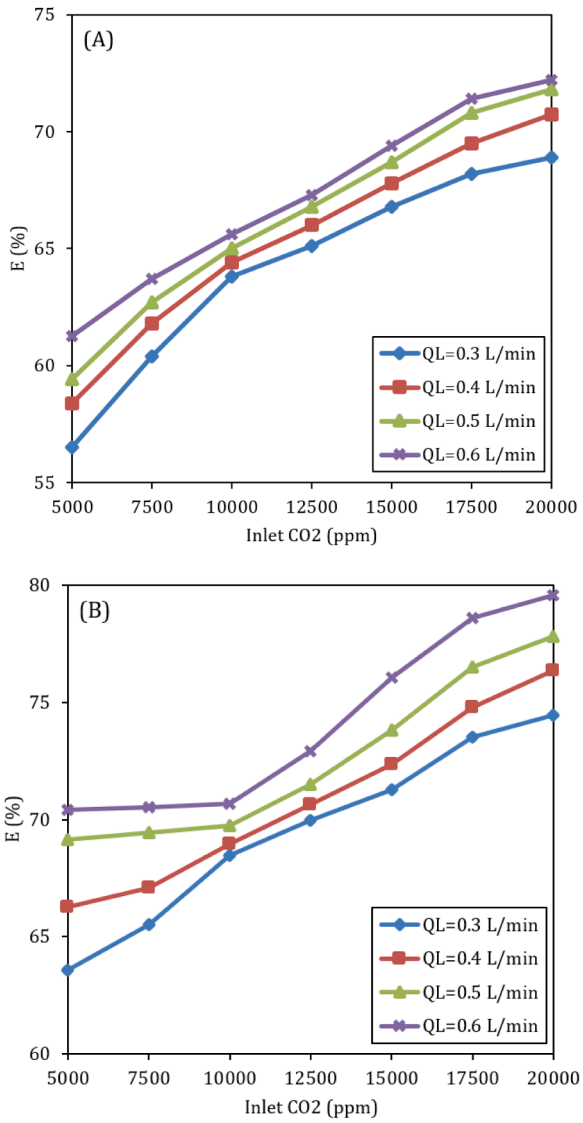


**Fig. 5.** Effect of $CO_2$ inlet concentrations **A)** MEA solution concentration = 1 M (RPB rotational speed = 900 rpm and $Q_G$ = 56 L/min) **B)** MEA solution concentration = 2 M, (RPB rotational speed = 900 rpm and $Q_G$ = 56 L/min).

### 3.4. Effect of inlet $CO_2$ concentration on $CO_2$ absorption

Fig. 5A and B show the effect of inlet $CO_2$ concentration on the Arc-RPB absorption efficiency with respect to rotational speed (900 rpm), liquid flow rates (0.3–0.6 Lit/min) and MEA concentrations (1 M and 2 M). Fig. 5A and B depict that increase in the inlet concentration of $CO_2$ from 5000 ppm until 20,000 ppm enhances absorption efficiency in all liquid flow rates. The increase in the absorption efficiency at this range is due to the enhancement of $CO_2$ concentration driving force between gas and liquid phases.

As Fig 5A and B show $CO_2$ absorption efficiency enhances with an increase in the MEA molar flow rate. With the enhancement of the liquid phase flow rate, the gas-liquid interface increases in the bed and enhances the RPB efficiency. It should be mentioned that the increase in the liquid phase flow rate does not significantly affect the RPB efficiency. So that, with an increase of about 66% in the liquid flow rate (from 0.3 $L/min$ to 0.5 $L/min$), the reactor efficiency enhanced by about 3%.

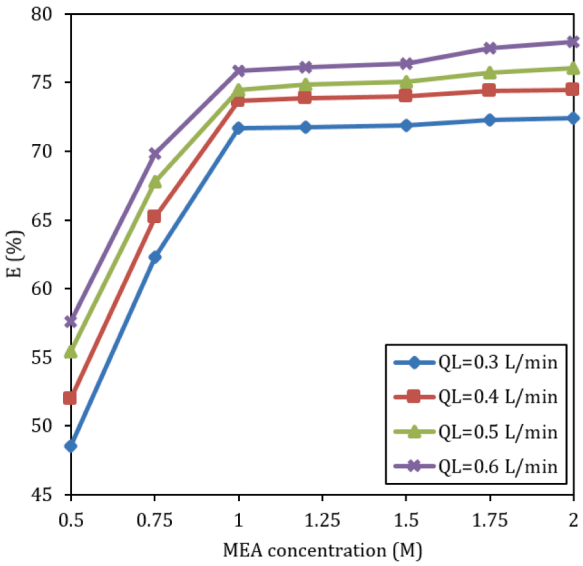


**Fig. 6..** Effect of MEA concentration on Arc-RPB efficiency at different liquid flow rates (RPB rotational speed = 900 rpm, $Q_G$ = 56 L/min and $CO_2$ inlet concentration = 20,000 ppm).

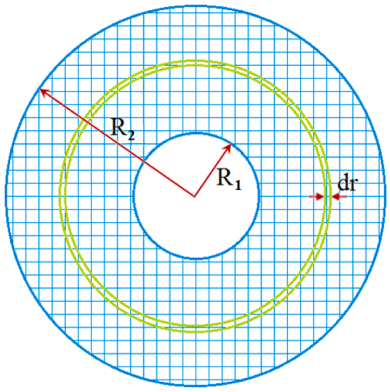


**Fig. 7..** Schematic of packing and control volume.

### 3.5. Effect of MEA concentration on $CO_2$ absorption

Fig. 6 shows the effect of MEA concentration on the Arc-RPB efficiency at the rotational speed of 900 rpm, $CO_2$ inlet concentration of 20,000 ppm, gas inlet flow rate of 56 lit/min and different liquid flow rates between 0.3–0.6 Lit/min. As Fig. 6 depicts, with increasing MEA concentration from 0.5 M to 2 M, the absorption efficiency enhances at all liquid flow rates. Results showed that enhancement of MEA solution concentrations from 0.5 M to 1 M significantly increased the absorption efficiency (about 20%) compared to that enhancement of MEA solution concentrations from 1 M to 2 M (less than 3% increase in the absorption efficiency). According to Yeh and Bai [38], the MEA liquid solution absorption capacity shows a low absorption capacity increase when concentration enhances more than 7%wt (over than 1 M). So, as Fig. 6 depicts $CO_2$ absorption efficiency shows very low increase (less than 3%) when MEA concentration enhances from 1 M to 2 M.

### 3.6. Development of $k_Ga$ correlation

In the process of $CO_2$ absorption with MEA solution, the interphase mass transfer rate $N_A$ can be expressed as [39]:

$$N_A = k_G(C - C_e) \tag{12}$$

**Table 2**
Gas mixture and liquid solutions properties.

| Fluid | $\mu$ $(kg/m.s)$ | $\rho$ $(kg/m^3)$ | $\sigma$ $(kg/s^2)$ |
|---|---|---|---|
| Gas mixture | $1.88 \times 10^{-5}$ | 1.19 | – |
| 0.5 M Liquid solution | $1.079 \times 10^{-3}$ | 1000 | $7.121 \times 10^{-2}$ |
| 1.0 M Liquid solution | $1.153 \times 10^{-3}$ | 1002 | $6.931 \times 10^{-2}$ |
| 1.5 M Liquid solution | $1.246 \times 10^{-3}$ | 1004 | $6.777 \times 10^{-2}$ |
| 2.0 M Liquid solution | $1.360 \times 10^{-3}$ | 1005 | $6.647 \times 10^{-2}$ |

where $k_G$, $C$ and $C_e$ are the gas-phase mass transfer coefficient, $CO_2$ inlet concentration and equilibrium $CO_2$ concentration at the gas-liquid interface, respectively. The mass transfer equation for $CO_2$ on a volumetric element of packing, Fig. 7, can be developed in the following form:

$$\frac{d(Q_G C)}{dr} = N_A a(2\pi rh) \tag{13}$$

where $a$ and $h$ are the special interfacial area between gas-liquid phases and the axial height of packing, respectively. In Eq. (13), the changes in the gas phase volumetric rate $Q_G$ due to the absorption of $CO_2$ were also omitted to simplify calculations [15,40–44] . Also, the maximum reduction in the gas phase volumetric rate due to the $CO_2$ absorption was less than 3% for current study experimental conditions. The combination of Eqs. (12) and (13) gives:

$$Q_G \frac{dC}{dr} = k_G a(C - C_e)(2\pi rh) \tag{14}$$

Due to very fast reaction between $CO_2$ and MEA solution [37], the equilibrium concentration of $CO_2$ in the gas-liquid interface can be supposed as zero ($C_e = 0$). So, Eq. (14) is simplified as:

$$Q_G \frac{dC}{C} = k_G a(2\pi rh)dr \tag{15}$$

The gas side overall volumetric mass transfer coefficient $k_G a$ is evaluated by the integration of Eq. (15). So, $k_G a$ is calculated by the following equation:

$$k_G a = \frac{Q_G}{\pi(R_2^2 - R_1^2)h} \ln \frac{C_2}{C_1} \tag{16}$$

where $C_1$, $C_2$, $R_1$ and $R_2$ are $CO_2$ concentration at the gas outlet, $CO_2$ concentration at the gas inlet, the inner diameter and the outer diameter of the packing zone, respectively.

In the current study, an attempt was made to provide a correlation for predicting of $k_G a$ by experimental data. This correlation is suggested as follows:

$$k_G a = A \times Re_G^{b_1} Re_L^{b_2} Gr_G^{b_3} We_L^{b_4} y_{in,CO_2}^{b_5} x_{in,MEA}^{b_6} \tag{17}$$

where $Re$, $Gr$, $We$, $y_{in,CO_2}$ and $x_{in,MEA}$ are Reynolds number, Grashof number, Weber number, the mole fraction of $CO_2$ at the gas inlet and the mole fraction of $MEA$ at the liquid inlet, respectively. Due to the effect of fluid concentration on fluid properties, the values of the fluids viscosity, density and surface tension in the dimensionless numbers were listed in Table 2.

To determine the optimal values of the constants of $A$, $b_1$, $b_2$, $b_3$, $b_4$, $b_5$ and $b_6$ in Eq. (17), Genetic-Algorithm (GA) was used in the current study. The average absolute relative error (AARE), Eq. (18), was implemented as an objective function of GA optimization problem as:

$$\text{AARE} = \left(\frac{1}{N}\left(\sum_{i=1}^{N}\left|\frac{k_G a_{experimental_i} - k_G a_{correlation\,i}}{k_G a_{experimental_i}}\right|\right)\right) \times 100 \tag{18}$$

Table 3 shows the optimal values of Eq. (17) constants and AARE value. Also, Fig. 8 depicts a parity plot between the experimental results and proposed correlation with respect to ±20% error lines. According to AARE value, it can be inferred that the proposed correlation predicts laboratory $k_G a$ with appropriate accuracy

### 3.7. Performance of Arc-RPB with other RPBs

Table 4 presents some information about the performance of different types of RPBs including absorption efficiency and $k_G a$ for $CO_2$ absorption by MEA solution. According to Table. 4, due to the different operational conditions in the reported experimental works, the comparison of Arc-RPB performance with the other RPBs in the literature were done on basis of gas handling capacity per volume of packing $(Q_G / V_{mesh})$ and $k_G a$. As Table. 4 presents, the small values of $k_G a$ and $Q_G / V_{mesh}$ were obtained for the Arc-RPB compared to other RPBs, but the efficiency of the Arc-RPB is relatively high. It can be concluded that although the $k_G a$ value in the Arc-RPB are relatively small, on the other hand, due to the high residence time of the gas phase which is equal to low values of $Q_G / V_{mesh}$, the Arc-RPB provides good efficiency for $CO_2$ absorption with MEA with respect to other RPBs.

## 4. Conclusion

In this research, a new design of RPB as Arc-RPB was presented by making fundamental changes in the geometry of the packing as the Arc-blades mesh and in the gas inlets section from conventional circle type into a rectangular shape. To investigate the Arc-RPB performance, $CO_2$ absorption efficiency was studied under different operating conditions with the MEA aqueous solutions. Experimental results showed that an

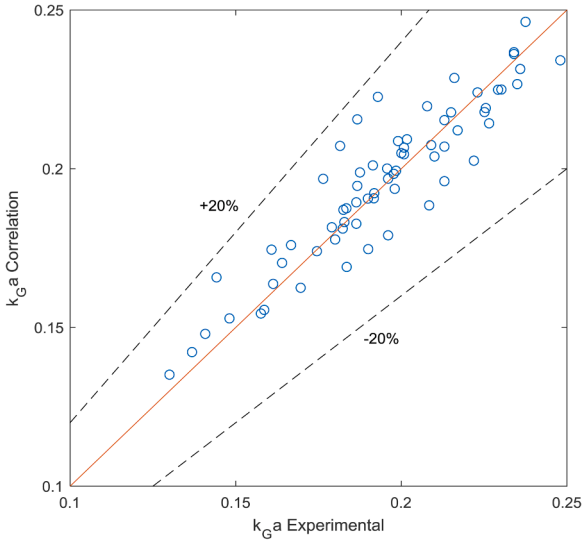


**Fig. 8..** Comparison of $k_G a$ for experimental data and proposed correlation (Eq. (17)).

**Table 3**
Evaluated constants of Eq. (17) by GA method and AARE value.

| $A = (a_t D_{CO_2-solution}) / d_p$ | b1 | b2 | b3 | b4 | b5 | b6 | AARE |
|---|---|---|---|---|---|---|---|
| 2.066 | 1.332 | 0.102 | 0.035 | 0.038 | 0.203 | 0.201 | 4.17% |

**Table 4**
Comparison of different RPBs performance in $CO_2$ absorption with MEA.

| RPB type (bed type) | $CO_2$ (% *Vol*) | MEA (% *wt*) | RPB rotational speed (*rpm*) | $Q_G/V_{mesh}(1/s)$ | $k_Ga(1/s)$ | Efficiency (%) | Ref. |
|---|---|---|---|---|---|---|---|
| Counter-current (xpamet mesh) | 15 | 30–90 | 600–1450 | 1.357 | 1.8 - 6.2 | Not available | [40] |
| Counter-current (wire mesh) | 10 | 30 | 600 | 1.606–3.212 | 1.8 - 3.1 | 44–84 | [41] |
| Co-counter current (perspex sheets) | 3.4–4.7 | 30–100 | 600–1000 | 6.774 | 0.64 - 7.11 | Not available | [45] |
| Cross-flow (wire mesh) | 0.02–1 | 10 | 540–1600 | 0.325–2.275 | 0.3 - 2.54 | 9.6–98 | [46] |
| Counter-current (wire mesh) | 10 | 1 | 600–1800 | 0.711–5.214 | 0.69 - 1.59 | <35 | [47] |
| | | | | 0.258–1.887 | 0.25 −0.84 | <30 | |
| | | | | 0.140–1.025 | 0.12 - 0.84 | <25 | |
| Counter-current (wire mesh) | 1–10 | 6–12 | 375–1735 | 0.236–0.702 | 0.5 - 0.75 | 35–75 | [48] |
| Counter-current (wire mesh) | 2 | 6 | 400–1600 | 1.906 | 0.3–0.7 | 15–29 | [49] |
| Counter-current (wire mesh) | 0.5–2 | 3–12 | 400–1600 | 0.169 | 0.13 - 0.23 | 49–78 | This work |

increase in Arc-RPB rotational speed from 300 to 900 rpm increases absorption efficiency about 9% for 1 M MEA solution and about 3% for 2 M MEA solution in the different liquid flow rates. Furthermore, the rate of change in the absorption efficiency for 2 M MEA solution was small compared to 1 M MEA solution in the range of 300 to 900 rpm. Also, results showed that for rotational speeds more than 900 rpm due to reduction in the residence time of the phases, the performance of the absorption efficiency reduces (less than 3%) at different MEA concentrations and liquid phase flow rates. Study of the different values of gas to liquid flow rate ratio $(Q_g/Q_l)$ showed that increase in the $Q_g/Q_l$ from 94 to 187 decreases absorption efficiency about 5% at different MEA solution concentrations. Reduction in the efficiency was due to a decrease in liquid phase holdup and gas-liquid interfacial area at the packing surface at high values of $Q_g/Q_l$.

With study the effect of $CO_2$ inlet concentration, results showed that increase in $CO_2$ concentration from 5000 ppm to 20,000 ppm enhances absorption efficiency about 12%. In addition, the effect of MEA solution concentration was investigated on the Arc-RPB performance. Results showed that an increase in MEA concentration from 0.5 M to 1 M increases absorption efficiency about 23% but, enhancement of MEA concentration from 1 M to 2 M has a weak effect (less than 2%) in absorption performance.

At the final part of this work, based on the experimental data a correlation was proposed to predict gas-phase volumetric mass transfer coefficient $(k_Ga)$. This correlation was in terms of effective dimensionless numbers in the RPBs. The constant of the correlation was evaluated by the Genetic Algorithm (GA) optimization method. The relative error between experimental data and correlation was achieved about 4.17%.

## Declaration of Competing Interest

The authors declare that they have no known competing financial interests or personal relationships that could have appeared to influence the work reported in this paper.

## Acknowledgement

The authors wish to acknowledge the financial support provided by the deputy of research and technology of Semnan University (Grant number 9801-01).

## References

[1] IEA, CO2 emissions from fuel combustion overview 2020, https://www.iea.org/reports/co2-emissions-from-fuel-combustion-overview (2020) 1–13.
[2] T. N.Borhani, M. Wang, Role of solvents in $CO_2$ capture processes: the review of selection and design methods, Renewable Sustainable Energy Rev. 114 (2019).
[3] Z. Zhang, T.N.G. Borhani, M.H. El-Naas, Carbon Capture, Exergetic, Energetic and Environmental Dimensions, 2018, pp. 997–1016.
[4] D.Y.C. Leung, G. Caramanna, M.M. Maroto-Valer, An overview of current status of carbon dioxide capture and storage technologies, Renewable Sustainable Energy Rev. 39 (2014) 426–443.
[5] D. Jansen, M. Gazzani, G. Manzolini, E.v. Dijk, M. Carbo, Pre-combustion CO2 capture, Int. J. Greenhouse Gas Control 40 (2015) 167–187.
[6] W.L. Theo, J.S. Lim, H. Hashim, A.A. Mustaffa, W.S. Ho, Review of pre-combustion capture and ionic liquid in carbon capture and storage, Appl. Energy 183 (2016) 1633–1663.
[7] E.S. Rubin, H. Mantripragada, A. Marks, P. Versteeg, J. Kitchin, The outlook for improved carbon capture technology, Prog. Energy Combust. Sci. 38 (2012) 630–671.
[8] R.S. Haszeldine, Carbon capture and storage: how green can black be? Science 325 (2009) 1647–1652.
[9] L. Zhu, China's Carbon Emission Report 2016, Harvard Kennedy School, Belfer Center for Science and International Affairs, Cambridge, MA, USA, 2016, pp. 1–44.
[10] E. Oko, M. Wang, A.S. Joel, Current status and future development of solvent-based carbon capture, Int. J. Coal. Sci. Technol. 4 (2017) 5–14.
[11] E. Oko, M. Wang, C. Ramshaw, Study of mass transfer correlations for rotating packed bed columns in the context of solvent-based carbon capture, Int. J. Greenhouse Gas Control 91 (2019).
[12] Z. Qian, Q. Chen, I.E. Grossmann, Optimal synthesis of rotating packed bed reactor, Comput. Chem. Eng. 105 (2017) 152–160.
[13] N. Chamchan, J.-Y. Chang, H.-C. Hsu, J.-L. Kang, D.S.H. Wong, S.-S. Jang, J.-F. Shen, Comparison of rotating packed bed and packed bed absorber in pilot plant and model simulation for CO 2 capture, J. Taiwan Inst. Chem. Eng. 73 (2017) 20–26.
[14] C. Ramshaw, R.H. Mallinson, Mass transfer process, US Patent No. 4283255 (1981).
[15] L. Xiang, L. Wu, L. Gao, J. Chen, Y. Liu, H. Zhao, Pilot scale applied research on $CO_2$ removal of natural gas using a rotating packed bed with propylene carbonate, Chem. Eng. Res. Des. 150 (2019) 33–39.
[16] H. Duan, K. Zhu, H. Lu, C. Liu, K. Wu, Y. Liu, B. Liang, $CO_2$ absorption performance in a rotating disk reactor using DBU-glycerol as solvent, Chin. J. Chem. Eng. (2019).
[17] Y.-M. Wang, Y.-S. Chen, Capture of $CO_2$ by highly concentrated alkanolamine solutions in a rotating packed bed, Environ. Prog. Sustain. Energy 38 (2019) e13263.
[18] L. Zhang, S. Wu, Y. Gao, B. Sun, Y. Luo, H. Zou, G. Chu, J. Chen, Absorption of $SO_2$ with calcium-based solution in a rotating packed bed, Sep. Purif. Technol. 214 (2019) 148–155.
[19] S. Bai, G.-W. Chu, S.-C. Li, H.-K. Zou, Y. Xiang, Y. Luo, J.-F. Chen, $SO_2$ Removal in a pilot scale rotating packed bed, Environ. Eng. Sci. 32 (2015) 806–815.
[20] Z. Qian, Z.-H. Li, K. Guo, Industrial applied and modeling research on selective $H_2S$ removal using a rotating packed bed, Ind Eng. Chem. Res. 51 (2012) 8108–8116.
[21] G.-W. Chu, Y. Luo, C.-Y. Shan, H.-K. Zou, Y. Xiang, L. Shao, J.-F. Chen, Absorption of $SO_2$ with ammonia-based solution in a cocurrent rotating packed bed, Ind. Eng. Chem. Res. 53 (2014) 15731–15737.
[22] Y. Ouyang, Y. Xiang, X.-Y. Gao, H.-K. Zou, G.-W. Chu, R.K. Agarwal, J.-F. Chen, Micromixing efficiency optimization of the premixer of a rotating packed bed by CFD, Chem. Eng. Process. 142 (2019).
[23] W. Jiao, Y. Liu, G. Qi, A new impinging stream–rotating packed bed reactor for improvement of micromixing iodide and iodate, Chem. Eng. J. 157 (2010) 168–173.
[24] X. Li, Y. Liu, Z. Li, X. Wang, Continuous distillation experiment with rotating packed bed, Chin. J. Chem. Eng. 16 (2008) 656–662.

[25] P.-F. Yang, S. Luo, D.-S. Zhang, P.-Z. Yang, Y.-Z. Liu, W.-Z. Jiao, Extraction of nitrobenzene from aqueous solution in impinging stream-rotating packed bed, Chem. Eng. Process. 124 (2018) 255–260.
[26] M. Emami-Meibodi, M. Soleimani, S. Bani-Najarian, Toward enhancement of rotating packed bed (RPB) reactor for $CaCO_3$ nanoparticle synthesis, Int. Nano Lett. 8 (2018) 189–199.
[27] C.-C. Lin, Y.-C. Lin, Preparation of ZnO nanoparticles using a rotating packed bed, Ceram. Int. 42 (2016) 17295–17302.
[28] J. Chen, L. Shao, Mass production of nanoparticles by high gravity reactive precipitation technology with low cost, China Particuol. 1 (2003) 64–69.
[29] J.-F. Chen, Y.-H. Wang, F. Guo, X.-M. Wang, C. Zheng, Synthesis of nanoparticles with novel technology: high-gravity reactive precipitation, Ind. Eng. Chem. Res. 39 (2000) 948–954.
[30] T.L. Chen, Y.K. Fang, S.L. Pei, S.Y. Pan, Y.H. Chen, P.C. Chiang, Development and deployment of integrated air pollution control, $CO_2$ capture and product utilization via a high-gravity process: comprehensive performance evaluation, Environ. Pollut. 252 (2019) 1464–1475.
[31] Y.-Z. Lu, W. Liu, Y.-C. Xu, Y. Luo, G.-W. Chu, J.-F. Chen, Initial liquid dispersion and mass transfer performance in a rotating packed bed, Chem. Eng. Process. 140 (2019) 136–141.
[32] L.-L. Zhang, J.-X. Wang, Y. Xiang, X.-F. Zeng, J.-F. Chen, Absorption of carbon dioxide with ionic liquid in a rotating packed bed contactor: mass transfer study, Ind. Eng. Chem. Res. 50 (2011) 6957–6964.
[33] P.V. Danckwerts, The reaction of $CO_2$ with ethanolamines, Chem. Eng. Sci. 34 (1979) 443–446.
[34] T.L. Donaldson, Y.N. Nguyen, Carbon dioxide reaction kinetics and transport in aqueous amine membranes, Ind. Eng. Chem. Fundam. 19 (1980) 260–266.
[35] A. Aboudheir, P. Tontiwachwuthikul, A. Chakma, R. Idem, Kinetics of the reactive absorption of carbon dioxide in high $CO_2$-loaded, concentrated aqueous monoethanolamine solutions, Chem. Eng. Sci. 58 (2003) 5195–5210.
[36] Y.S. Yu, Y. Li, H.F. Lu, L.W. Yan, Z.X. Zhang, G.X. Wang, V. Rudolph, Multi-field synergy study of $CO_2$ capture process by chemical absorption, Chem. Eng. Sci. 65 (2010) 3279–3292.
[37] A. Aroonwilas, A. Veawab, P. Tontiwachwuthikul, Behavior of the mass-transfer coefficient of structured packings in $CO_2$ absorbers with chemical reactions, Ind. Eng. Chem. Res. 38 (1999) 2044–2050.
[38] A.C.C. Yeh, H. Bai, Comparison of ammonia and monoethanolamine solvents to reduce $CO_2$ greenhouse gas emissions, Sci. Total Environ. 228 (1999) 121–133.
[39] J.-L. Kang, K. Sun, D.S.-H. Wong, S.-S. Jang, C.-S. Tan, Modeling studies on absorption of $CO_2$ by monoethanolamine in rotating packed bed, Int. J. Greenhouse Gas Control 25 (2014) 141–150.
[40] J. Lee, T. Kolawole, P. Attidekou, Carbon capture from a simulated flue gas using a rotating packed bed adsorber and mono ethanol amine (MEA), Energy Procedia 114 (2017) 1834–1840.
[41] C.-H. Yu, H.-H. Cheng, C.-S. Tan, $CO_2$ capture by alkanolamine solutions containing diethylenetriamine and piperazine in a rotating packed bed, Int. J. Greenhouse Gas Control 9 (2012) 136–147.
[42] C.-C. Lin, C.-R. Chu, Mass transfer performance of rotating packed beds with blade packings in carbon dioxide absorption into sodium hydroxide solution, Sep. Purif. Technol. 150 (2015) 196–203.
[43] P. Sandilya, D.P. Rao, A. Sharma, G. Biswas, Gas-phase mass transfer in a centrifugal contactor, Ind. Eng. Chem. Res. 40 (2001) 384–392.
[44] Y. Liu, F. Zhang, D. Gu, G. Qi, W. Jiao, X. Chen, Gas-phase mass transfer characteristics in a counter airflow shear rotating packed bed, Can. J. Chem. Eng. 94 (2016) 771–778.
[45] M.S. Jassim, G. Rochelle, D. Eimer, C. Ramshaw, Carbon dioxide absorption and desorption in aqueous monoethanolamine solutions in a rotating packed bed, Ind. Eng. Chem. Res. 46 (2007) 2823–2833.
[46] C.-C. Lin, B.-C. Chen, Carbon dioxide absorption in a cross-flow rotating packed bed, Chem. Eng. Res. Des. 89 (2011) 1722–1729.
[47] C.-C. Lin, Y.-W. Kuo, Mass transfer performance of rotating packed beds with blade packings in absorption of $CO_2$ into MEA solution, Int. J. Heat Mass Transf. 97 (2016) 712–718.
[48] C.-C. Lin, W.-T. Liu, C.-S. Tan, Removal of carbon dioxide by absorption in a rotating packed bed, Ind. Eng. Chem. Res. 42 (2003) 2381–2386.
[49] M. Shirzadi Ahou Dashti, M. Abolhasani, Intensification of $CO_2$ capture by monoethanolamine solution containing $TiO_2$ nanoparticles in a rotating packed bed, Int. J. Greenhouse Gas Control 94 (2020).